

Violation of Bell's inequality for phase singular beams

Shashi Prabhakar,^{*} Salla Gangi Reddy,[†] A Aadhi,[‡] Chithrabhanu P,[§] and R. P. Singh[¶]

Physical Research Laboratory, Navrangpura, Ahmedabad. 380009, India.

(Dated: December 6, 2024)

We have considered optical beams with phase singularity and experimentally verified that these beams, although being classical, have properties of two mode entanglement observed in quantum optics. We have observed violation of Bell's inequality for continuous variables experimentally using the Wigner function proposed by Chowdhury et. al. [Phys. Rev. A **88**, 013830 (2013)]. It uses correlations in position-momentum space through Wigner distribution function.

PACS numbers: 42.50.Tx, 42.25.Kb, 42.60.Jf, 03.65.Ud

I. INTRODUCTION

Optical vortex is observed as a dark spot in bright background. Being topological structures, they are robust and find applications in free space and fiber communication [1]. For the vortex of topological charge n , the azimuthal phase variation is $2\pi n$ in a full rotation around the dark spot [2]. The sense of rotation of phase provides the sign of its charge. The topological charge n can be considered as an important parameter for such beams. One of the main characteristics of these beams is that each photon carry an orbital angular momentum (OAM) of $n\hbar$ [3]. The OAM carrying property has raised extensive interest in scientific community due to its unique applications in the fields of particle manipulation [4] and quantum information [5–7].

Optical vortex beams of higher order have been experimentally realized both in laser [8] as well as electron beams [9, 10]. These beams form an infinite dimensional basis for applications such as quantum computation and cryptography [5, 11]. One can encode large amount of information with higher order optical vortices due to the increase in entropy with the order of vortex [12].

Study of the Wigner distribution function (WDF) has been found to be very useful since it can provide coherence information in terms of the joint position and momentum (phase-space) distribution for a particular optical field [13]. Using WDF, one can study the non-classical correlations present in classical beams. Recently, the famous Bell's inequality has been defined for classical sources using WDF and it has been shown theoretically that the optical vortex beams violate this inequality [14]. These non-local continuous variable correlations exist between the position and momentum. Such quantum inspired inseparability has been termed as “classical entanglement” [15, 16].

In this article, we have demonstrated the experimental verification of “classical entanglement” using the WDF

and two-point Bell's inequality for optical vortex beams obtained in ref. [14]. To verify the theoretical results, we produce different orders of vortex fields described by the LG modes using a spatial light modulator (SLM) [17]. The two-point correlation function has been found using the interference between vortices of the same order and is scanned using a shearing Sagnac interferometer (SSI) [18, 19]. Theory related to this study has been discussed in section II, experimental details have been given in section III. Results and discussion constitute in section IV and finally we conclude in section V.

II. THEORETICAL BACKGROUND

The electric field of an optical vortex of order n and centered at origin can be written as

$$E_{nm}(r, \phi, z) = \frac{C_{nm}^{LG}}{w(z)} \left(\frac{r\sqrt{2}}{w(z)} \right)^{|n|} \exp\left(-\frac{r^2}{w^2(z)}\right) L_m^{|n|} \left(\frac{2r^2}{w^2(z)} \right) \exp\left(ik \frac{r^2}{2R(z)}\right) \exp(in\phi) \times \exp[i(2m + |n| + 1)\zeta(z)], \quad (1)$$

where $L_m^{|n|}$ is the generalized Laguerre polynomial, the radial index $m > 0$ and the azimuthal index is n . C_{nm}^{LG} is the normalization constant, $w(z)$, $R(z)$ and $\zeta(z)$ are beam parameters and r , ϕ are radial and azimuthal coordinates in space respectively. Such beams contain azimuthal phase dependence of $\exp(in\phi)$ and singularity at the center.

A. Wigner Distribution Function

The WDF for optical vortex beams can be written as [13, 20]

$$W_{nm}(X, P_X; Y, P_Y) = \frac{(-1)^{n+m}}{\pi^2} L_n[4(Q_0 + Q_2)] \times L_m[4(Q_0 - Q_2)] \exp(-4Q_0), \quad (2)$$

^{*} shaship@prl.res.in

[†] sgreddy@prl.res.in

[‡] aadhi@prl.res.in

[§] chithrabhanu@prl.res.in

[¶] rpsingh@prl.res.in

where $\{X, P_X\}$ and $\{Y, P_Y\}$ are conjugate pairs of dimensionless quadratures. Q_0 and Q_2 are

$$\begin{aligned} Q_0 &= \frac{1}{4} [X^2 + P_X^2 + Y^2 + P_Y^2], \\ Q_2 &= \frac{XP_Y - YP_X}{2}, \end{aligned} \quad (3)$$

where the scaled variables X , P_X , Y and P_Y can be defined as

$$\begin{aligned} x(y) &\rightarrow \frac{w}{\sqrt{2}} X(Y), \\ p_x(p_y) &\rightarrow \frac{\sqrt{2}\lambda}{w} P_X(P_Y) \end{aligned} \quad (4)$$

and follow $[\hat{X}, \hat{P}_X] = [\hat{Y}, \hat{P}_Y] = i$.

B. Bell's inequality for continuous variable systems

For discrete entangled systems, the Bell-CHSH inequality can be written as [21, 22]

$$B = |S(a, b) + S(a, b') + S(a', b) - S(a', b')| < 2, \quad (5)$$

where (a, b) , (a', b') are two analyser settings. The entanglement in quantum systems with continuous variables is characterized by probabilities. For continuous variable systems, WDF is expressed as an expectation value of a product of displaced parity operators. Banaszek and Wodkiewicz [23, 24] have argued that the WDF can be used to derive the analog of Bell's inequality in continuous variable systems.

Considering the transformation $\Pi(X, P_X, Y, P_Y) = \pi^2 W(X, P_X, Y, P_Y)$ in dimensionless quadratures, then the Bell-CHSH inequality B with chosen points $\{a, b\} \equiv \{X_1, P_{X_1}, Y_1, P_{Y_1}\}$ and $\{a', b'\} \equiv \{X_2, P_{X_2}, Y_2, P_{Y_2}\}$ can be written as

$$\begin{aligned} B &= \Pi_{nm}(X_1, P_{X_1}, Y_1, P_{Y_1}) + \Pi_{nm}(X_1, P_{X_1}, Y_2, P_{Y_2}) \\ &\quad + \Pi_{nm}(X_2, P_{X_2}, Y_1, P_{Y_1}) \\ &\quad - \Pi_{nm}(X_2, P_{X_2}, Y_2, P_{Y_2}) < 2. \end{aligned} \quad (6)$$

C. Bell's violation for first order vortex ($n=1$ and $m=0$)

From Eq. 2, the WDF of an optical vortex beam with topological charge 1 can be obtained as

$$W_{10}(X, P_X, Y, P_Y) = e^{-X^2 - P_X^2 - Y^2 - P_Y^2} \times \frac{(P_X - Y)^2 + (P_Y + X)^2 - 1}{\pi^2}. \quad (7)$$

Choosing $X_1 = 0, P_{X_1} = 0, X_2 = X, P_{X_2} = 0, Y_1 = 0, P_{Y_1} = 0, Y_2 = 0, P_{Y_2} = P_Y$, the Bell-CHSH parameter can be written as

$$\begin{aligned} B &= \Pi_{10}(0, 0, 0, 0) + \Pi_{10}(X, 0, 0, 0) \\ &\quad + \Pi_{10}(0, 0, 0, P_Y) - \Pi_{10}(X, 0, 0, P_Y) \end{aligned} \quad (8)$$

$$\begin{aligned} &= e^{-P_Y^2} (P_Y^2 - 1) + e^{-X^2} (X^2 - 1) - \\ &\quad e^{-P_Y^2 - X^2} [(P_Y + X)^2 - 1] - 1. \end{aligned} \quad (9)$$

The maximum Bell's violation considering only two variables X and P_Y is $|B_{max}| \sim 2.17$ which occurs at $X \sim 0.45$ and $P_Y \sim 0.45$. Considering all eight variables from Eq. 6, the maximum Bell's violation is $|B_{max}| \sim 2.24$ at $X_1 \sim -0.07, P_{X_1} \sim 0.05, X_2 \sim 0.4, P_{X_2} \sim -0.26, Y_1 \sim -0.05, P_{Y_1} \sim -0.07, Y_2 \sim 0.26$ and $P_{Y_2} \sim 0.4$. The experimental verification for these results have been discussed in the following section.

III. EXPERIMENTAL SETUP

The experimental setup to find the two-point correlation function (TPCF) is shown in Fig. 1. Computer generated holography has been used to generate optical vortices [25]. A Gaussian laser beam from an intensity stabilized He-Ne laser (Spectra-Physics, 117A) is incident normally to the SLM (Holoeye, LC-R 2500) using the mirror M1 and the beam splitter BS1. The SLM is a liquid-crystal-based device that can modulate light and can be used as a dynamic diffractive optical element. Vortices of different orders are produced in the first diffracted order by introducing different fork patterns onto the SLM via a computer PC1. Apertures A1 and A2 are used to select an optical vortex of the desired order. A polarizer (P) is used to fix the polarization (here vertical) of the optical vortex. The vortex with the vertical polarization is coupled to the Shearing-Sagnac interferometer (SSI) that comprises the beam splitter BS2 and two mirrors, M2 and M3. A quarter-wave plate (QWP) and a half-wave plate (HWP) are kept in common path for the quadrature selection. A glass block mounted upon a rotation stage is also kept in the common path to introduce the shear in two transverse directions. This arrangement ensures that both the clockwise (cw) and the counter-clockwise (ccw) fields experience one reflection from and one transmission through the beam splitter. This removes the effect of deviations from 50% transmission and polarization-sensitivity of the beam splitters.

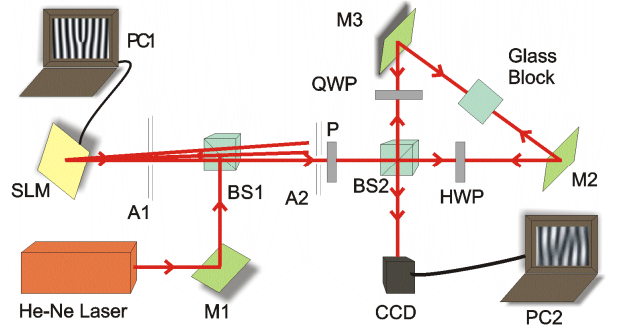


FIG. 1. (Color online) Experimental setup for determination of TPCF.

The two counter-propagating beams are interfered and imaged using a Evolution VF cooled CCD camera that is connected to computer PC2.

First, we have calibrated the shear in laser-beam produced by the glass block. For this, we put one polarizer inside the SSI. The clock-wise and counter clock-wise propagation of beams were chosen by the rotation of the polarizer. We have put a normal grating on the SLM to propagate Gaussian beam inside the SSI. Then, we rotate the glass block such that there is no shear between the two beams. After this, we have provided some shear in the glass block which is mounted on a rotation stage with linear scale. The shear is varied in equal steps. The particular rotation in the glass block will provide us the shear in the beams propagating inside the SSI. We have recorded the intensity of two beams with CCD camera. These images were processed in MATLAB to determine the shear in between the two beams. The beam width w of the laser beam falling on the CCD was determined using the 2D curve-fitting in MATLAB. The scaled shear was obtained using Eq. 4 corresponding to the linear scale on the rotation stage of glass block. We have achieved the required shears after calibrating the SSI. The amount of shear as a function of scale has been shown in Fig. 2.

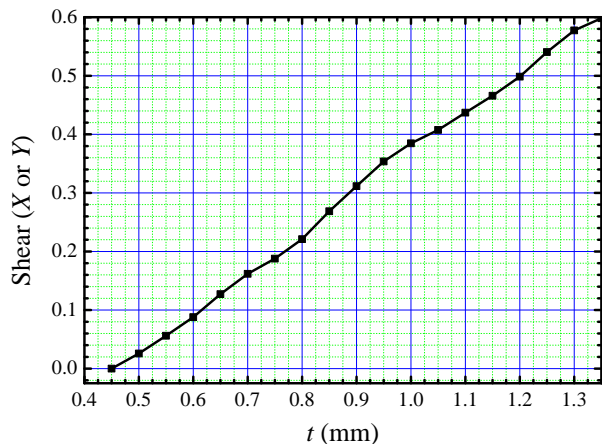


FIG. 2. (Color online) Calibration curve for dimensionless shear (X, Y) in the SSI. The x -axis (t) denotes the position on linear scale present on the mount on which the cube was mounted.

IV. RESULTS

The main component of our experiment is to determine the TPCF [12, 18]. At the particular position of rotation of glass block, we have recorded the interferograms by keeping the fast axes of the QWP and the HWP parallel to the incident beams' polarization direction. In this orientation, the wave plates have no effect on the polarization of the optical beam, and both the

cw and ccw propagating fields travel equal optical path lengths inside SSI. The recorded interferograms contain the information of $\text{Re}[\Phi(X, Y, R_1, R_2)]$. Measurement of $\text{Im}[\Phi(X, Y, R_1, R_2)]$ is achieved by rotating HWP by $\pi/4$, resulting in a $3\pi/4$ optical delay between the counter-propagating fields. Keeping the lateral shear values the same, another set of interferograms are recorded which contain the $\text{Im}[\Phi(X, Y, R_1, R_2)]$. Fig. 3(a) and 3(b) show the TPCF of Gaussian beam and optical vortex of topological charge 1 respectively. These TPCFs are obtained at zero shears ($X=0, Y=0$). To obtain the TPCF at different shears (X, Y), the glass cube is rotated to corresponding positions along x and y axes suggested by Fig. 2.

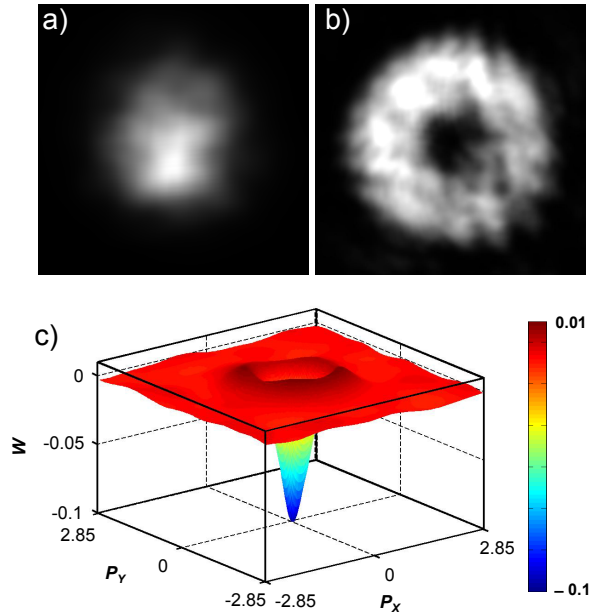


FIG. 3. (Color online) Experimentally obtained TPCF for a) Gaussian beam and b) optical vortex (right) beam for $n=1, m=0, X, Y=0$. c) WDF of an optical vortex for $n=1, m=0, X=0, Y=0$.

To obtain WDF, we have taken the Fourier transform (FT) of TPCF [13]. Fig. 3(c) shows the WDF of an optical vortex for $n=1$ and $m=0$ obtained at $X = Y = 0$, corresponding TPCF is shown in Fig. 3(b). This shows that our results are consistent with the previously obtained WDFs [13]. After obtaining four WDFs at chosen shears (X_1, Y_1), (X_2, Y_1), (X_1, Y_2) and (X_2, Y_2), the four dimensional addition was performed over $P_{X1}, P_{X2}, P_{Y1}, P_{Y2}$ axes to determine B as defined in Eq. 6. The experimentally obtained WDF is a two-dimensional (P_X, P_Y) function, keeping two dimensions (X, Y) to be constant. However, after addition of four WDFs, the dimension for B is a four-dimensional function ($P_{X1}, P_{X2}, P_{Y1}, P_{Y2}$) and other four dimensions (X_1, X_2, Y_1, Y_2) are fixed. Equation 6 shows the generation of a four-dimensional matrix after adding four two-dimensional functions. Proper axes should be considered

while adding. The maximum value of B was determined to verify the violation of Bell's inequality.

Considering $X_1=0$, $P_{X1}=0$, $X_2=X$, $P_{X2}=0$, $Y_1=0$, $P_{Y1}=0$, $Y_2=0$, $P_{Y2} = P_Y$, the 2D surface plot of $|B|$ varying with X and P_Y described by Eq. 8 is shown in Fig. 4. The $|B_{max}|$ obtained from Fig. 4 is 2.1793, which indicates that the continuous variables of optical vortex field are non-separable or correlated. From the plot, location of the maximum of $|B|$ has been determined that matches with the theory.

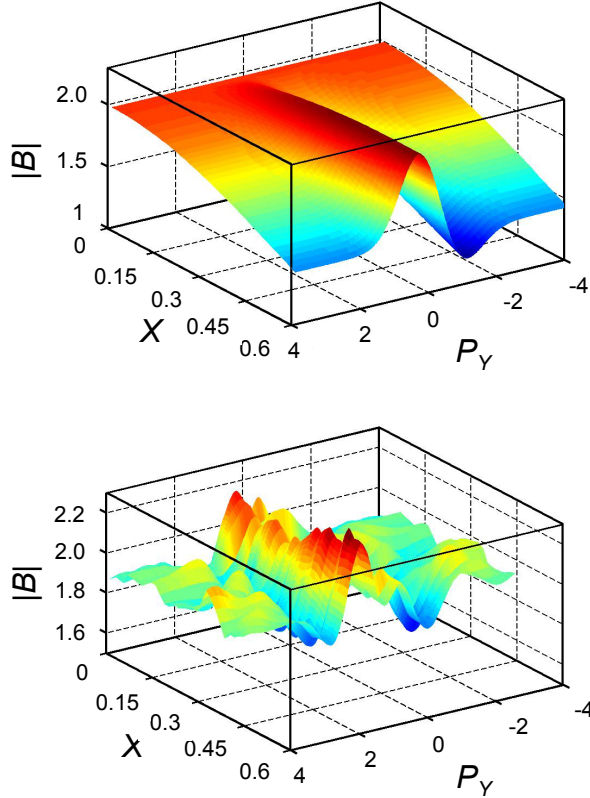


FIG. 4. (Color online) Variation of $|B|$ with X and P_Y (Eq. 8) for $n = 1$ and $m = 0$. Theoretical (top) and experimental (bottom).

Figure 5 shows the variation maximum Bell's inequality violation ($|B_{max}|$) for Gaussian beam and optical vortices of order $n=1-3$, $m = 0$. From the Fig. 5, it is clear that there is no Bell's inequality violation for Gaussian beam. However for optical vortex beams, the Bell's inequality has been violated. The amount of Bell's violation increases with the increase in order of the vortices. The amount of non-local correlations increases with the

order of an optical vortex due to the increase in Bell's violation parameter (B_{max}). To estimate the experimental error, the experiment was repeated for five times. In every set of experiment, four WDFs were determined and for each WDF, two sets of interferograms corresponding to real and imaginary component of TPCF were recorded. $|B_{max}|$ was calculated for each set of experiments. The $|B_{max}|$ used in Fig. 5 is the average of five $|B_{max}|$ determined from each set of experimental interferograms. Errors are the standard deviations for five values of all the $|B_{max}|$.

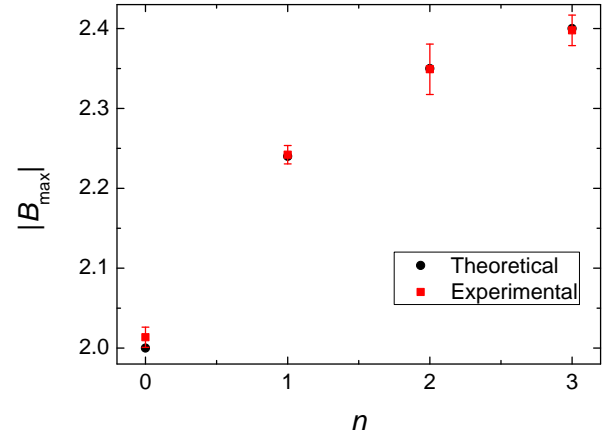


FIG. 5. (Color online) Variation of $|B_{max}|$ with the order of vortex (n) and $m = 0$.

V. CONCLUSIONS

We have experimentally verified the quantum inspired optical entanglement of classical optical vortex beams which have topological singularities. We have experimentally found that these classical beams violate Bell's inequality for continuous variable. The extent of violation of Bell's inequality increases with the increase in its topological charge. To obtain this, we have used the coherence properties, two-point correlation function and Wigner distribution function of such beams. The violation of Bell's inequality in phase-space ($x, p_x; y, p_y$) clearly shows the existence of different spatial correlation properties for optical vortices, which is similar to entanglement in quantum systems. This type of entanglement can be seen with electron vortex beams also due to the generic nature of vorticity, having far-reaching implications.

[1] N. Bozinovic, Y. Yue, Y. Ren, M. Tur, P. Kristensen, H. Huang, A. E. Willner, and S. Ramachandran, *Terabit-scale orbital angular momentum mode division multiplex-*

ing in fibers, Science **340**, 1545–1548 (2013).
 [2] L. Allen, S. M. Barnett, and M. J. Padgett, *Optical angular momentum* (Institute of Physics, 2003).

- [3] L. Allen, M. Beijersbergen, R. Spreeuw, and J. Woerdman, *Orbital angular momentum of light and the transformation of laguerre-gaussian laser modes*, Physical Review A **45**, 8185–8189 (1992).
- [4] D. G. Grier, *A revolution in optical manipulation*, Nature **424**, 810–816 (2003).
- [5] A. Mair, A. Vaziri, G. Weihs, and A. Zeilinger, *Entanglement of the orbital angular momentum states of photons*, Nature **412**, 313316 (2001).
- [6] G. Molina-Terriza, J. P. Torres, and L. Torner, *Twisted photons*, Nature Physics **3**, 305–310 (2007).
- [7] R. Horodecki, M. Horodecki, and K. Horodecki, *Quantum entanglement*, Reviews of Modern Physics **81**, 865–942 (2009).
- [8] R. Fickler, R. Lapkiewicz, W. N. Plick, M. Krenn, C. Schaeff, S. Ramelow, and A. Zeilinger, *Quantum entanglement of high angular momenta*, Science **338**, 640–643 (2012).
- [9] B. J. McMorran, A. Agrawal, I. M. Anderson, A. A. Herzing, H. J. Lezec, J. J. McClelland, and J. Unguris, *Electron vortex beams with high quanta of orbital angular momentum*, Science **331**, 192–195 (2011).
- [10] J. Verbeeck, H. Tian, and P. Schattschneider, *Production and application of electron vortex beams*, Nature **467**, 301–304 (2010).
- [11] W. Tittel, J. Brendel, H. Zbinden, and N. Gisin, *Quantum cryptography using entangled photons in energy-time bell states*, Physical Review Letters **84**, 4737–4740 (2000).
- [12] A. Kumar, S. Prabhakar, P. Vaity, and R. P. Singh, *Information content of optical vortex fields*, Optics Letters **36**, 1161 (2011).
- [13] R. Pratap Singh, S. Roychowdhury, and V. Kumar Jaiswal, *Wigner distribution of an optical vortex*, Journal of Modern Optics **53**, 1803–1808 (2006).
- [14] P. Chowdhury, A. S. Majumdar, and G. S. Agarwal, *Nonlocal continuous-variable correlations and violation of bell’s inequality for light beams with topological singularities*, Physical Review A **88**, 013830 (2013).
- [15] K. H. Kagalwala, G. Di Giuseppe, A. F. Abouraddy, and B. E. A. Saleh, *Bell’s measure in classical optical coherence*, Nature Photonics **7**, 72–78 (2012).
- [16] C. V. S. Borges, M. Hor-Meyll, J. A. O. Huguenin, and A. Z. Khoury, *Bell-like inequality for the spin-orbit separability of a laser beam*, Physical Review A **82**, 033833 (2010).
- [17] J. Curtis and D. Grier, *Structure of optical vortices*, Physical Review Letters **90**, 133901 (2003).
- [18] C. Iaconis and I. A. Walmsley, *Direct measurement of the two-point field correlation function*, Optics Letters **21**, 1783 (1996).
- [19] C.-C. Cheng, M. G. Raymer, and H. Heier, *A variable lateral-shearing sagnac interferometer with high numerical aperture for measuring the complex spatial coherence function of light*, Journal of Modern Optics **47**, 1237–1246 (2000).
- [20] R. Simon and G. S. Agarwal, *Wigner representation of laguerre-gaussian beams*, Optics Letters **25**, 1313 (2000).
- [21] J. S. Bell, *On the einstein-podolsky-rosen paradox*, Physics **1**, 195–200 (1964).
- [22] J. Clauser, M. Horne, A. Shimony, and R. Holt, *Proposed experiment to test local hidden-variable theories*, Physical Review Letters **23**, 880–884 (1969).
- [23] K. Banaszek and K. Wdkiewicz, *Direct probing of quantum phase space by photon counting*, Physical Review Letters **76**, 4344–4347 (1996).
- [24] K. Banaszek and K. Wdkiewicz, *Nonlocality of the einstein-podolsky-rosen state in the wigner representation*, Physical Review A **58**, 4345–4347 (1998).
- [25] A. V. Carpentier, H. Michinel, J. R. Salgueiro, and D. Olivieri, *Making optical vortices with computer-generated holograms*, American Journal of Physics **76**, 916 (2008).